IET Nanobiotechnology

Research Article

IET Journals
The Institution of Engineering and Technology

Nigella sativa oil entrapped polycaprolactone nanoparticles for leishmaniasis treatment

ISSN 1751-8741
Received on 6th February 2018
Revised 11th May 2018
Accepted on 25th June 2018
E-First on 25th September 2018
doi: 10.1049/iet-nbt.2018.5115
www.ietdl.org

Emrah Sefik Abamor[1] ✉, Ozlem Ayse Tosyali[1], Melahat Bagirova[1], Adil Allahverdiyev[1]

[1]*Bioengineering Department, Yildiz Technical University, Esenler, Istanbul, Turkey*

✉ *E-mail: esabamor@gmail.com*

Abstract: This study is the first to investigate the antileishmanial activities of Nigella sativa oil (NSO) entrapped poly-ε-caprolactone (PCL) nanoparticles on *Leishmania infantum* promastigotes and amastigotes in vitro. NSO molecules with variable initial doses of 50, 100, 150, and 200 mg were successfully encapsulated into PCL nanoparticles identified as formulations NSO1, NSO2, NSO3, and NSO4, respectively. This process was characterised by scanning electron microscope, dynamic light scattering, Fourier transform infrared, encapsulation efficiency measurements, and release profile evaluations. The resulting synthetised nanoparticles had sizes ranging between 200 and 390 nm. PCL nanoparticles encapsulated 98% to 80% of initial doses of NSO and after incubation released approximately 85% of entrapped oil molecules after 288 h. All investigated formulations demonstrated strong antileishmanial effects on *L. infantum* promastigotes by inhibiting up to 90% of parasites after 192 h. The tested formulations decreased infection indexes of macrophages in a range between 2.4- and 4.1-fold in contrast to control, thus indicating the strong anti-amastigote activities of NSO encapsulated PCL nanoparticles. Furthermore, NSO-loaded PCL nanoparticles showed immunomodulatory effects by increasing produced nitric oxide amounts within macrophages by 2–3.5-fold in contrast to use of free oil. The obtained data showed significant antileishmanial effects of NSO encapsulated PCL nanoparticles on *L. infantum* promastigotes and amastigotes.

1 Introduction

Leishmaniasis is one of the most important and neglected tropical diseases in the world. It is caused by Leishmania parasites and the disease is transmitted to humans by the bites of infected sandflies. The bites cause mild to severe painful skin lesions, called cutaneous leishmaniasis (CL) or deadly visceral disorders classified as visceral leishmaniasis (VL). It is estimated that approximately 300 million people are at risk of being afflicted by leishmaniasis. Currently, 0.5 million cases of VL and 1.5–2 million cases of CL cases are reported annually worldwide. Annually, VL causes nearly 60,000 deaths all over the world [1–3]. Due to global warming, climate changes, wars, and migrations, it is predicted that each form of the disease will rapidly become widely distributed to most currently non-epidemic regions [4–8]. Since there is no safe and reliable vaccine against leishmaniasis, chemotherapy has in the past been used to treat the disease [9]. However, current antileishmanial drugs have several disadvantages such as toxicity, long-term administration, resistance, and high cost that restrict their use in clinical applications [10, 11]. Therefore, it is very critical to develop new antileishmanial formulations in order to fight against the disease.

In recent years, there has been a growing interest in the use of natural products, especially those isolated from plants for the treatment of infectious diseases [12, 13]. It is predicted that approximately 25% of drugs that are used in the treatment of diseases is obtained from herbal products [14]. Herbal oils are accepted as the most important natural products and are frequently used in developing new medicines to eradicate infectious diseases. Since these oils include extensive mixtures of bioactive molecules and possess hydrophobic features, they are considered as effective inhibitory agents against a broad spectrum of microorganisms such as bacteria, fungi, viruses, and parasites.

Although their action mechanisms on infectious agents are still unclear, it is suggested that herbal oils disrupt microbial cellular membranes and leads to oxidative stress due to their hydrophobic and lipophilic features [15–19]. One example is Nigella sativa oil (NSO), which is isolated from the seeds of the *N. sativa* plant. This plant is known as one of the most promising herbal products because it contains several strong bioactive compounds, notably thymoquinone. NSO is promising due to its abundant active components, and anti-oxidant, anti-inflammatory, anti-cancerogenic, antimicrobial, and immunostimulatory features [20–23]. Several studies have found that NSO provides some antileishmanial activities through its active component, thymoquinone [24].

In our previous paper, we indicated that combinations of NSO with TiAgNps enhanced the antileishmanial efficacies of the oil while decreasing its toxicity [25]. Despite their excellent antimicrobial features, applications of vegetable oils are clinically restricted due to decreased stability and toxicity [26, 27]. The oil is particularly dependent on low water solubility, and vegetable oils are vulnerable to environmental factors such as moisture, pH, and oxygen and may be also degraded within living systems.

In order to augment stability, bioactivity and also protect bioactive molecules from degradation, they have recently been encapsulated into nanoparticulate delivery systems. This encapsulation process can also provide regulation of drug release and also decrease toxicity [28]. Poly-ε-caprolactone (PCL) is a hydrophobic polymer that is composed of one polar ester and five non-polar methylene groups. It is usually prepared by a ring opening polymerisation technique from caprolactone monomers [29]. PCL nanoparticles possess special features such as high permeability, bioavailability, biodegradability, and non-toxicity, which make them ideal structures for synthetising drug delivery systems [30, 31]. Moreover, since it is approved by the United States Food and Drug Administration, the application of PCL nanoparticles in clinics has recently attracted the interest of researchers.

In particular, the hydrolysis of ester linkages within the human body provides degradation of the polymer and a sustained/controllable release of drugs [32]. Utilising the various features of PCL nanoparticles, they have been used to deliver drugs into desired regions of the body to fight against various diseases [33]. However, to our knowledge, there have been no previous studies in the literature investigating the antimicrobial behaviours of PCL nanoparticles loaded with bioactive molecules such as NSO.

By considering the strong antimicrobial profiles of NSO and significant roles of PCL nanoparticles in regards to delivery, sustained release and protection drugs from degradation, we propose that encapsulation of NSO into PCL nanoparticles may increase the bioactivities and antimicrobial features of this oil and also reduce its toxicity. Taking into consideration our previous study and the antiparasitic actions of NSO, we suggest that NSO encapsulated PCL nanoparticulate formulation may exhibit excellent antileishmanial activities. Therefore, the main goal of the present study is to prepare NSO entrapped PCL nanoparticles by a single emulsion method, to characterise the synthetised nanoparticles with various techniques, and also to investigate their antileishmanial activities against *Leishmania infantum* promastigotes and amastigotes in vitro.

2 Materials methods

2.1 Materials

PCL (MW 14,000), polyvinyl alcohol (PVA) (average MW 30,000–70,000), Methylthiazolyltetrazolium (MTT) were purchased from Sigma-Aldrich (St. Louis, MO). Dichloromethane (DCM), sodium nitrite, sulphanilamide, naphthylethylenediamide dihydrochloride were obtained from Merck (Darmstadt, Germany). Roswell Park Memorial Institute medium (RPMI 1640) was purchased from GIBCO (Life Technologies, USA). Nigella sativa fixed oil (Zade Vital) was commercially obtained from a national pharmacy. A mouse J774 macrophage cell line was obtained from the Histology and Embryology Department, Istanbul University, Istanbul, Turkey. Ultra-pure water was obtained from a Millipore MilliQ Gradient system.

2.2 Preparation of NSO-PCL nanoparticles

PCL nanoparticles were prepared by an o/w single solvent evaporation technique. Briefly, 200 mg of PCL was dissolved in 5 ml of DCM. Then different initial doses of NSO such as 50, 100, 150, and 200 mg were added into the organic phase and were identified as NSO1, NSO2, NSO3, and NSO4, respectively. The organic phase was added into 25 ml of an aqueous phase containing PVA as a stabiliser. The organic phase and aqueous phase were emulsified for 5 min with a probe sonicator (Bandelin Sonopuls, Germany) in an ice bath. Complete evaporation of DCM from the emulsion (o/w) was performed by stirring for 4 h. Nanoparticle suspensions were centrifuged at 14,000 rpm for 30 min. The obtained pellet was washed twice with deionised distilled water. The final pellet was re-suspended in a trehalose solution (2% w/v) as a cryoprotectant and the solution was then lyophilised for 48 h.

2.3 Characterisation of nanoparticles

2.3.1 Particle size and zeta potential: Particle size and the polydispersity index were identified by photon correlation spectroscopy (PCS) by using a Zetasizer Nano ZS (Malvern Instruments, Malvern, UK). Size measurements were performed in triplicate following preparation of nanoparticle suspensions by diluting in distilled water at a ratio of 1/100 (*v*/*v*) at 25°C. The polydispersity index range was comprised between 0 and 1. The zeta potentials of diluted synthetised nanoparticles were measured by using the same instrument at 25°C.

2.3.2 Scanning electron microscopy: Freeze-dried nanoparticles were fixed on metallic studs like a thin film using adhesive tape and then coated with gold under vacuum. The particles were visualised by using an Evo LS10 (Zeiss, Welwyn Garden City, UK) scanning electron microscope (SEM) at an accelerating voltage of 10–20 kV.

2.3.3 Fourier transform infrared spectroscopy: Fourier transform infrared spectroscopy (FTIR) spectra were collected using an IR-Prestige 21 (Shimadzu, Japan) with an attenuated total reflectance technique. The FTIR spectrum of the PCL and NSO-PCL NPs was carried out in a region from 600 to 4000 cm^{-1}. Spectra were measured at 4 cm^{-1} resolution by scanning 16 times.

2.3.4 Encapsulation efficiency measurements: The supernatant was collected from the ultracentrifugation of nanoparticles and subjected for NSO quantification by using UV-Vis spectroscopy. Since thymoquinone, the most abundant compound of NSO, was monitored at a λ_{max} of 254 nm, the amount of encapsulated NSO into PCL nanoparticles was measured by using spectra at this wavelength. The quantification was done in triplicate for each formulation. The NSO concentrations in the supernatant were determined by using a standard calibration curve of NSO at various concentrations. The concentration of encapsulated oil was measured indirectly by calculating the differences between the prior concentrations of the oil used (50, 100, 150, and 200 mg/ml) and the concentration of free oil in the supernatant. The encapsulation efficiency (EE) and loading capacity of NSO was evaluated by using the following formulas: (see equation below)

2.3.5 In vitro drug release studies: Fifteen milligrams of oil-loaded PCL nanoparticles were dispersed in 3 ml of phosphate-buffered saline (PBS) at pH 7.4. Then suspensions were incubated in a shaker at 37°C. At appropriate intervals, test solutions were centrifuged at 12,000 rpm for 20 min and 1 ml of supernatant was used for the analysis. The amounts of released NSO within the supernatants were evaluated by UV spectrophotometer at 254 nm.

2.4 L. infantum promastigote culture

L. infantum parasites were grown in RPMI-1640 supplemented with 10% heat-inactivated FBS at 27°C. Metacyclic promastigotes were harvested at the late log phase following 120 h incubation.

2.5 J774 macrophage cell culture

J774 macrophage cells were cultured in RPMI 1640 (supplemented with 100 U/ml penicillin and 100 IU/ml streptomycin) including 10% (v/v) heat-inactivated FBS. Then cells were incubated at 37°C in an incubator with 5% CO_2.

2.6 Cell viability assay

J774 macrophage cells were seeded into 96-well plates at a density of 104 cells/well and incubated for 24 h to allow cell attachment. The cells were then exposed to free NSO, free PCL nanoparticles, and NSO-loaded PCL nanoparticles at various concentrations varying between 50 and 1000 µg/ml for 144 h. Untreated cells were used as positive control. Following incubation, the formulations were replaced with medium containing an MTT reactant (10 mg/ml) and the cells were then incubated for 4 h. Afterwards, DMSO was put into each well in order to dissolve the formazan crystals. Absorbance was measured at 570 nm using a microplate reader (Thermo Scientific, Multiskan FC).

2.7 Determination of promastigote growth inhibition

In order to evaluate the antileishmanial effects of the nanoparticles and free oil, studies were performed on an *L. infantum* promastigote culture. For that purpose, promastigotes in a log phase were seeded into a 24-well plate at a density of 5×104 parasites/ml. After overnight incubation at 27°C, different concentrations of free NSO and NSO encapsulated PCL nanoparticles at concentrations of 50, 100, 250, 500, and 1000 µg/ml were added into wells. Each concentration was tested in

$$\text{Encapsulation efficiency}\% = (\text{a mount of encapsulated oil})/(\text{initial amount of oil}) \times 100$$

$$\text{Oil loading capacity}\% = (\text{entrapped oil})/(\text{nanoparticles weight}) \times 100$$

triplicate. Treated promastigotes were incubated at 27°C for 192 h. The number of viable promastigotes for each group was counted with a haemocytometer at different time intervals (72, 144, and 192 h). Briefly, a 50 µl *L. infantum* promastigote culture was obtained from each well and mixed with 2% formalin at a ratio of 1:10. Then suspensions were put into a haemocytometer, and the slide was investigated in an inverted microscope (Olympos CKX 41). IC50 values of all the samples were determined by finding the concentration that inhibited half of the promastigotes.

2.8 Screening of anti-amastigote efficacies

In order to find the anti-amastigote activities of tested formulations, 1.5 × 104 J774 cells were inoculated into six-well plates. Following overnight incubation, macrophages were infected with 1.5 × 105 stationary phase *L. infantum* promastigotes in order to obtain an amastigote-macrophage culture. After 4 h incubation at 37°C, non-internalised promastigotes were removed by washing the plates in triplicate with PBS. Infected macrophages were treated with different concentrations of free NSO and NSO-PCL NPs (50, 100, 250, 500, and 1000 µg/ml) and plates were then incubated for 192 h. Afterwards, cells were fixed with methanol for 10 min and then stained with Giemsa for 3 min. Later, all wells of the plates were rinsed with PBS and slides within the wells were removed from the plates to monitor in an inverted microscope at 100× dimensions.

The infection index of all specimens was evaluated by counting the infected cell number and intracellular Leishmania parasites randomly chosen in 200 cells. By dividing the number of infected macrophages with the number of all macrophages in the zone, % infectivity value was assessed.

2.9 Measurement of nitric oxide production

Nitric oxide production by macrophages was performed by the Griess reaction as previously described [34]. Briefly, 1 × 106 macrophages/ml were inoculated in 24-well cell culture plates prior to 24 h incubation. Then, the medium was discharged and fresh medium containing individually different concentrations of free oil, empty NPs, and NSO-PCL NPs (50,100, 250, 500, or 1000 µg/ml) were added into all plates. After 192 h incubation, supernatants were collected and the amounts of released NO from macrophages were analysed by a Griess reaction method. In this method, 50 µL supernatant and serial dilutions of sodium nitrite standard solution (0.5–100 µM) were placed into 96-well plates and then mixed with 50 µL of the Griess reagent (combination of 1% sulphanilamide, 0.1% naphthylethylenediamide dihydrochloride, and 2.5% H_3PO_4). After incubation for 10 min at room temperature, absorbance values were measured in an ELISA reader at 570 nm. The amounts of nitrite within each well were quantified based on a standard curve.

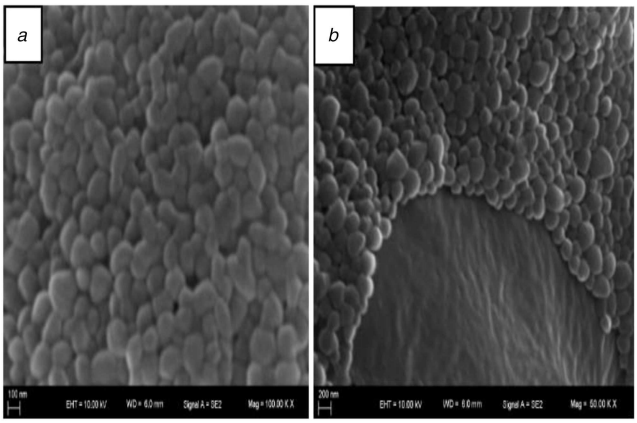

Fig. 1 *SEM images of synthetised nanoparticles*
(a) empty, ***(b)*** NSO encapsulated PCL nanoparticles (NSO4 formulation)

2.10 Statistical analysis

The results were expressed as mean ± SD. Statistical Packages of Social Sciences (SPSS 16.0 version for Windows) software with parametric tests (paired samples *t*-test, analysis of variance, and Tukey's post-hoc test) were used for statistical analysis. A $P < 0.05$ value was considered statistically significant.

3 Results

3.1 SEM analysis

Fig. 1 shows SEM images of empty and oil encapsulated PCL nanoparticles. The images in the figure show that synthetised nanoparticles exhibited spherical, uniform, and smooth shapes. Furthermore, there was a narrow size distribution for each formulation range between 200 and 400 nm. The NSO4 formulation had larger sizes than empty nanoparticles, thus indicating that the NSO4 formulation was loaded with oil molecules.

3.2 Size distribution and zeta potential analysis

Table 1 shows the dynamic light scattering (DLS) results of synthetised formulations including empty and NSO encapsulated PCL nanoparticles. The mean sizes of the nanoparticles were measured as 202, 212, 232, 350, and 389 nm for empty NP, NSO1, NSO2, NSO3, and NSO4 formulations, respectively. The size of the nanoparticles raised directly along with an increase in the amount of encapsulated oil molecules. Among the investigated formulations, free nanoparticles had the smallest size, while the size of the NSO4 nanoparticles, which included the largest amounts of NSO oil molecules, was about two times larger than free nanoparticles.

Table 1 also represents the PDI values and zeta potentials of all formulations. The PDI results varied between 0.12 and 0.2. This indicates that all of the synthetised nanoparticles possess a narrow size distribution. The zeta potentials of the nanoparticles varied between −4.92 and −8.29 mV. The negative zeta potentials of synthetised nanoparticles are attributed to a carboxylic end group of the PCL polymer.

3.3 Fourier transform infrared spectroscopy

FTIR spectroscopy was used in order to elucidate the presence of NSO within PCL nanoparticles. The liquid form of NSO bands and lyophilised empty PCL NPs and NSO-PCL NPs FTIR bands are shown in Fig. 2. Empty PCL NPs band at 2943 and 2868 cm^{-1} are assigned to C–H hydroxyl groups asymmetric and symmetric stretching, respectively. The band at 1724 cm^{-1} is assigned to –C=O stretching vibrations due to the ester carbonyl group. The band at 1238 cm^{-1} belongs to C–O–C asymmetric stretching.

The characteristic NSO spectrum present at a wavelength of 3007 cm^{-1} comes from the matching of the free NSO, empty PCL,

Table 1 Illustration of mean size, PDI values, zeta potential measurements, encapsulation efficiency, and reaction yield percentages of empty nanoparticles, NSO1, NSO2, NSO3, and NSO4 formulations

Formulation names	Size, nm	PDI	Zeta potential, mV	Encapsulation efficiency, %	Reaction yield, %
free NPs	202 ± 24	0.080	−4.92 ± 0.88	—	—
NSO1	212 ± 17	0.101	−6.57 ± 0.70	98.6	40.7
NSO2	232 ± 31	0.124	−6.34 ± 0.89	98.8	48.6
NSO3	350 ± 42	0.139	−7.85 ± 0.65	80.5	57.4
NSO4	389 ± 37	0.164	−8.29 ± 1.04	71.6	51.2

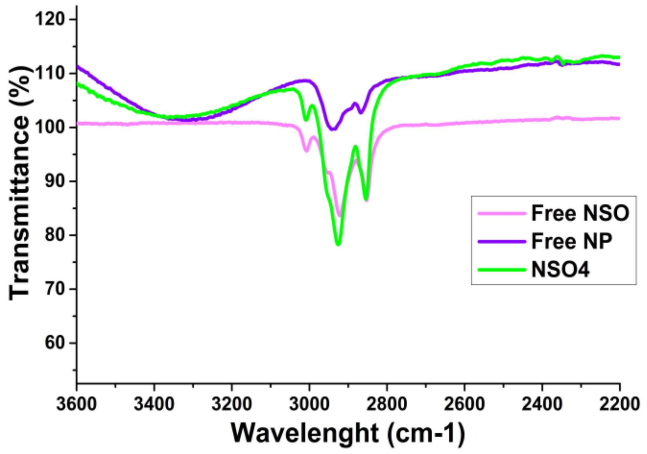

Fig. 2 *FTIR spectrum of the free NSO, Empty PCL NPs, and NSO-PCL NPs*

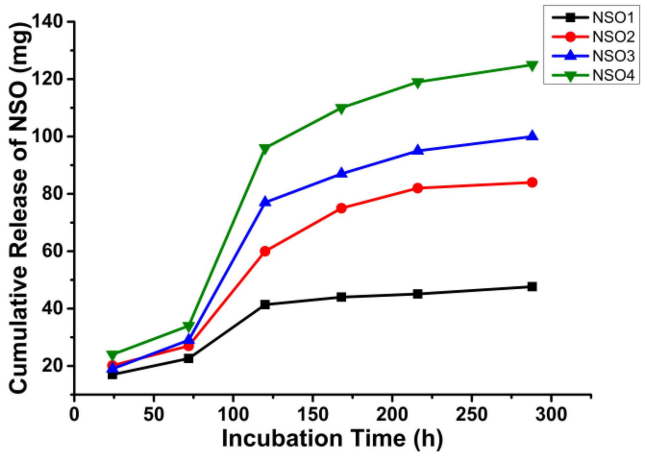

Fig. 3 *In vitro release profiles of NSO encapsulated PCL nanoparticles and cumulative release amounts of oil from NSO1, NSO2, NSO3, and NSO4 formulations*

and loaded PCL-NPs spectra. This peak was attributed to the stretching vibrations of C–H in CH=CH. Reduced intensity at 3007 cm^{-1} was observed due to the small concentration on the surface of the nanoparticles. This shows successfully encapsulation of NSO in PCL.

3.4 Encapsulation efficiency

Table 1 also demonstrates EE and reaction yield ratios of all synthetised oil entrapped PCL nanoparticles. As indicated, EE amounts were measured as 98.6, 98.8, 80.5, and 71.6% for the NSO1, NSO2, NSO3, and NSO4 formulations, respectively. It was determined that encapsulation efficiencies were diminished by an increase in initial oil amounts during the encapsulation process.

3.5 In vitro release study

The release profiles of PCL nanoparticulate formulations that consisted of different initial amounts of NSO were investigated for 288 h. Fig. 3 illustrates the cumulative increase of released oil amounts during the mentioned incubation time. The figure shows that the release of oil molecules from NSO-loaded nanoparticles was slower in the first three days. However, released NSO amounts enhanced rapidly due to a rapid degradation of nanoparticulate systems at time intervals following 72 h. The NSO1 formulation released approximately 94% of encapsulated oil molecules after 288 h incubation, while it was only 34% at the end of 72 h. Similarly, released oil amounts from the NSO2 formulation was 22.3 and 93.7 mg which corresponds to the ratio of 24 and 94% at the time intervals of 72 and 288 h, respectively. The NSO3 formulation released nearly 85% of the encapsulated oil at the end

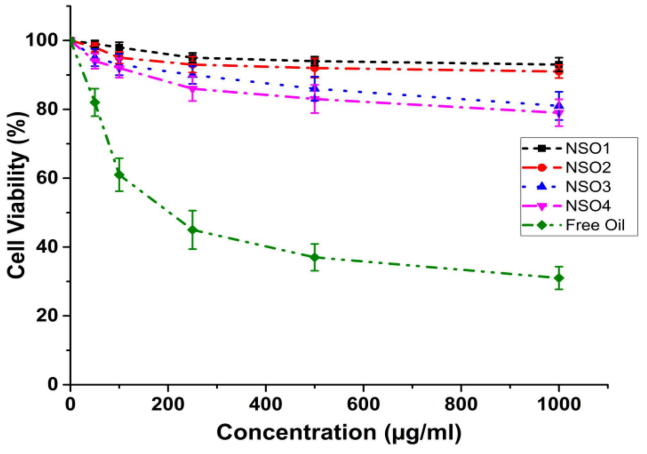

Fig. 4 *Cytotoxicity analysis of free oil and NSO encapsulated PCL nanoparticles on J774 macrophage cells following to 144 h incubation*

of the 288 h incubation period, while this ratio was measured as only 30% after 72 h incubation. Similarly, the amounts of released molecules from the NSO4 formulation increased with time. It was nearly 35% at the end of 72 h and then reached 90% after 288 h incubation.

3.6 Cytotoxicity analysis

Before investigating the antileishmanial activities of all synthetised nano-formulations, their cytotoxicities were screened on J774 macrophage cells by using an MTT method. In experiments, cells were exposed to different concentrations of each formulation ranging between 50 and 1000 µg/ml. No cytotoxic effect was observed for any of the synthetised nanoparticulate systems. The IC50 values of each formulation were higher than 1000 µg/ml. Among tested formulations, only NSO3 and NSO4 lead to an approximately 20% decrease in viabilities of macrophages when a 1000 µg/ml concentration was performed on cells at an incubation time of 144 h. These results reveal that all formulations at variable concentrations could be used in promastigote or a particularly amastigote-macrophage culture since no cytotoxicity was found on J774 macrophage cells. On the other hand, it was shown that free NSO oil at increased concentrations elicited cytotoxicity against J774 macrophage cells (Fig. 4). The IC50 value of NSO for macrophages was 125 µg/ml. These results support the determined that encapsulation of NSO into PCL nanoparticles prevents their toxicities on macrophages.

3.7 Anti-promastigote assay

All investigated formulations exhibited significant antileishmanial effects dependent on increased concentrations and exposure time. In Figs. 5–7, variable inhibitory activities of NSO1, NSO2, NSO3, and NSO4 formulations and free oil were illustrated at different concentrations ranging between 50 and 1000 µg/ml at various time intervals such as 72, 144, and 192 h. Fig. 5 shows that after 72 h incubation none of the nanoparticulate formulations showed remarkable inhibitory activities on *L. infantum* promastigotes. When only the highest concentrations were applied, there was at most a nearly 20% decrease in promastigote growth. In comparison, free NSO oil decreased the growth kinetics of Leishmania parasites after 72 h incubation. The anti-promastigote efficacies of free oil as augmented by an increase in concentration. When the lowest concentration of the oil (50 µg/ml) was applied, there was a 42% reduction in promastigote amounts, and this decrease reached 80% with administration of 1000 µg/ml free oil for 72 h.

The antileishmanial effectiveness of nanoparticulate formulations also increases depending on incubation times. Fig. 6 shows parasitic growth inhibition rates with 144 h incubation. Similar to 72 h incubation, the most significant effect was observed when parasites were exposed to free oil as this caused a nearly 85% inhibition in parasite growth rates. Another significant result is that

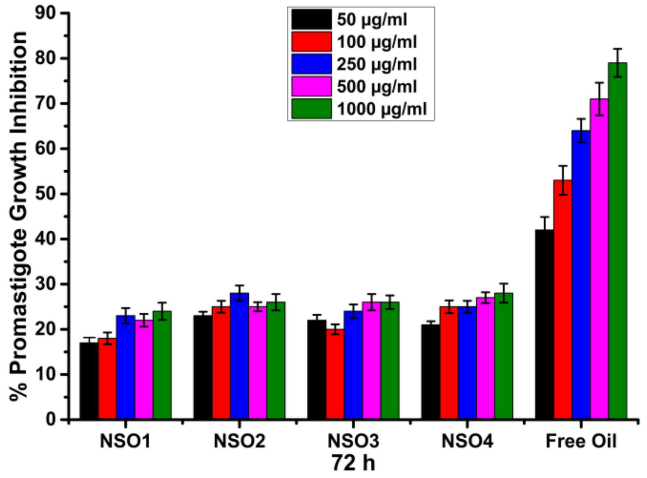

Fig. 5 *Growth inhibition percentages of L. infantum promastigotes that are exposed to NSO1, NSO2, NSO3, NSO4 formulations, and free oil for 72 h*

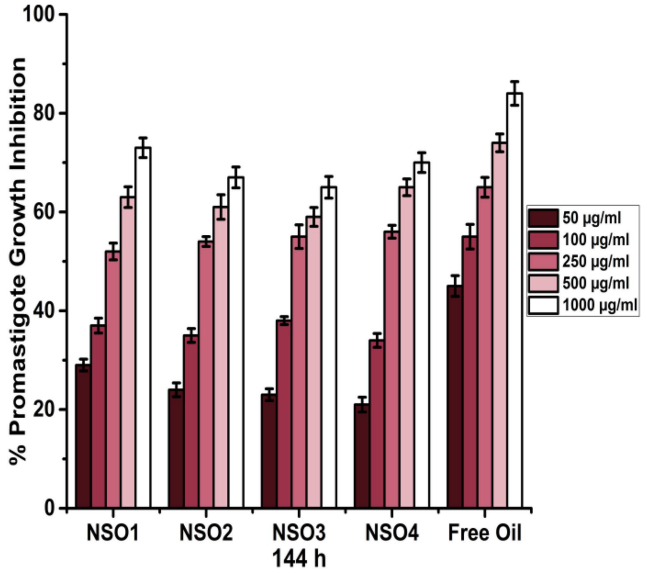

Fig. 6 *Growth inhibition percentages of L. infantum promastigotes that are exposed to NSO1, NSO2, NSO3, NSO4 formulations, and free oil for 144 h*

antileishmanial activities of oil-loaded nanoparticles considerably improved at the end of 144 h incubation in contrast to 72 h incubation. Each nanoparticulate formulation leads to an approximate 30% inhibition in promastigote growth at a 50 µg/ml concentration and this rate reached 70% with a 1000 µg/ml concentration of the formulation.

The most tremendous effect was seen when promastigotes were exposed to NSO1, NSO2, NSO3, and NSO4 formulations for 192 h (Fig. 7). Nearly 82% of promastigotes were inhibited following their exposure to a concentration of 1000 µg/ml. The IC50 value of NSO1 was 195 µg/ml. Similarly, after 192 h exposure to the highest concentration, the NSO2 formulation killed 84% of *L. infantum* promastigotes and its IC50 value was 175 µg/ml. Similar results were obtained when promastigotes were treated with various concentrations of NSO3 and NSO4 formulations ranging between 50 and 1000 µg/ml for 192 h.

Exposure to lower concentrations such as 50 and 100 µg/ml was not meaningfully effective against promastigotes for each time interval. However, the application of concentrations higher than 100 µg/ml leads to extreme inhibition of *L. infantum* parasites, especially at the end of 192 h. NSO3 and NSO4 formulations eliminated nearly 90% of *L. infantum* promastigotes when a concentration of 1000 µg/ml was used. IC50 values were 167 and 159 µg/ml for NSO3 and NSO4 formulations, respectively.

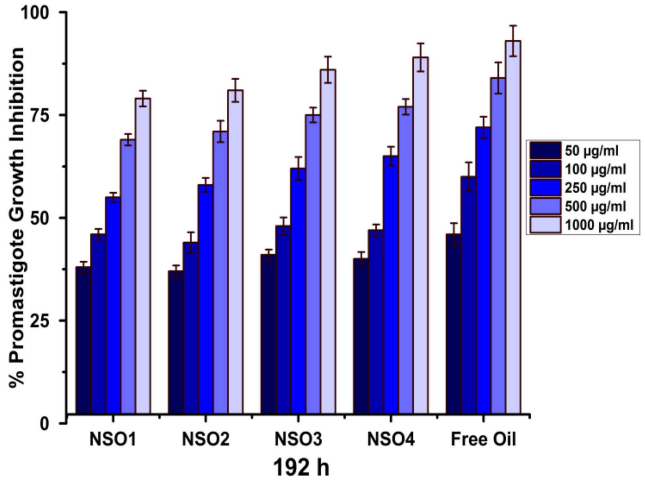

Fig. 7 *Growth inhibition percentages of L. infantum promastigotes that are exposed to NSO1, NSO2, NSO3, NSO4 formulations, and free oil for 192 h*

Similar to other time intervals, free oil demonstrated the most remarkable effect on promastigotes at the end of 192 h incubation since exposure to free oil resulted in inhibition of more than 90% of *L. infantum* parasites with an IC50 value of 125 µg/ml. On the contrary, this was obviously determined from the results that each oil-loaded PCL nano-formulation extremely inhibited parasitic growth along with an increase in incubation time, but their anti-promastigote activity was not remarkably effective at the earlier investigated time intervals, such as 72 h. This enhanced anti-promastigote efficacy indicates increased degradation rates of PCL nanoparticles which facilitated the release of oil molecules with the passage of time.

3.8 Anti-amastigote assay

As the antileishmanial activities of investigated formulations on promastigotes increased by exposure time, we only investigated anti-amastigote efficacies of formulations at a time interval of 192 h. Fig. 8 illustrates the antileishmanial effects of different concentrations of synthetised oil encapsulated PCL nanoparticulate formulations on *L. infantum* amastigotes via infection index analysis in a comparison with free oil molecules and also empty nanoparticles. Free nanoparticles did not show any inhibitory effects on *L. infantum* amastigotes. On the other hand, it was demonstrated that each formulation substantially decreased infection index ratios of macrophages infected with parasites. The other important point that must be emphasised is anti-amastigote activities of formulations were largely increased dependent on concentrations. When the highest concentrations were applied, dramatical reductions in infection indexes were recorded independently of formulation types.

The most significant effect was observed when the parasites were exposed to 1000 µg/ml NSO4. It was determined that exposure to a mentioned concentration of NSO4 resulted in approximately 4.5-fold decrease in infection index values in contrast to control. This was followed by NSO3, NSO2, and NSO1 with variable reductive effects ranging between 3.8 and 2.6 folds when compared with the control. IC50 values were measured as 165, 143, 115, and 102 µg/ml for NSO1, NSO2, NSO3, and NSO4 formulations, respectively, indicating that NSO4 formulation elicited the most significant anti-amastgiote efficacy following to 192 h incubation. Furthermore, the anti-amastigote efficacy of free NSO oil was also illustrated in Fig. 8. As it was shown, free oil exhibited superior antileishmanial effects on amastigotes when compared with oil-loaded PCL nanoparticles. Following free oil exposure, infection index values of macrophages diminished almost 5-fold in contrast to control. IC50 values of free oil on *L. infantum* amastigotes were measured as 95 µg/ml. These results revealed that oil encapsulated nanoparticulate formulations especially NSO3 and NSO4 elicited strong anti-amastigote

efficacies and their effectivenesses were close to the administration of free oil.

3.9 Evaluation of nitric oxide amounts

In the last step of our experiments, we studied on detection of released nitric oxide amounts from macrophages that were exposed to various concentrations of NSO1, NSO2, NSO3, and NSO4 formulations, free PCL nanoparticles and free oil molecules varying between 50 and 1000 µg/ml for 192 h. As it is indicated in Table 2, all investigated samples improved the amounts of released nitric oxide from J774 macrophage cells, in contrast, to control dependent on increased sample concentrations. Table 2 clearly illustrates that NSO encapsulated PCL nanoparticles supremely stimulated macrophages to generate higher levels of nitric oxide in contrast to free nanoparticles and free oil. Application of non-encapsulated free NSO leads to 1.6-fold enhancement at most in released nitric oxide amounts similar as free nanoparticles. On the other hand, oil entrapped PCL nanoparticulate formulations lifted produced amounts of nitric oxide in a range between 1.25 and 3 folds according to applied concentration. The most significant effect was seen when macrophages were treated with NSO4 formulation at the concentration of 1000 µg/ml. At this concentration, nanoparticle application resulted in approximately 3-fold increase in released nitric oxide amounts. This was followed by an NSO3 formulation which leads to a 2.8-fold rise of nitric oxide amounts at the same concentration. It was also determined that the amounts of released nitric oxide amounts from macrophages exposed to NSO1 and NSO2 formulations were not as much as NSO3 and NSO4, but was nevertheless higher than macrophages treated with free nanoparticles and oil.

4 Discussion

Because of their rich contents, vegetable oils exhibited strong antibacterial, antiviral, antifungal, anti-oxidant, anti-cancerogenic, and anti-inflammatory effects [35–37]. Due to these multifunctional features, herbal oils can be used in various fields like pharmaceutical industries, food chemistry, agriculture, and dentistry. A limitation, however, is that since these oils comprise unstable functional groups, their applications in biological systems are problematic. Likewise, herbal oils demonstrate poor aqueous solubility which results in a decrease in the bioavailabilities of these bioactive molecules [38–41]. Another important factor that restricts the use of essential oils in clinics is their toxicities. In various research, essential oils caused cytotoxicity for kidney, liver, blood, and spleen cells [42–44].

Thus, in order to improve bioavailabilities, decrease toxicities, and enhance biological activities, researchers have recently focused on the encapsulation of herbal oils into micro/nanoparticulate systems. These systems also provide the delivery of these bioactive molecules into desired regions of the body and prevent degradation by blood enzymes during their transportation within the bloodstream [38, 45, 46]. PCL nanoparticles have attracted the attention of scientists in the field of drug/vaccine delivery along with their major roles acting as scaffolds in tissue engineering applications.

PCL is a biocompatible, bioavailable, non-toxic polymer that can easily penetrate through vital barriers in the human body at nano-scales and can implement controllable and sustained release of drug molecules into targeted cells, tissues or organs [47–50]. In the literature, there are several studies demonstrating the encapsulation of essential oils and their components into PCL nanoparticles. Choi *et al.* successfully achieved encapsulation of eugenol into PCL nanoparticles by an emulsion-diffusion method. They demonstrated that up to 99% encapsulation was obtained thru this engulfment process that protected eugenol from light oxidation [51]. In another study, Ephrem *et al.* succeeded in entrapment of rosemary essential oils into PCL nanoparticles with a mean size of 220 nm and extremely high encapsulation efficacies up to a ratio of 99% [52]. In recent research, Thonggoom *et al.* investigated EE values and release profiles of clove essential oil encapsulated into amphiphilic polyethyleneglycol block polycaprolactone nanoparticles by using various molecular weights of PCL and different concentrations of essential oil. EE percentages of nanoparticles changed between 54.8 and 73.0. Moreover, released amounts of clove essential oil reached 70% after ten days of incubation. The authors suggested the high potential of oil encapsulated PCL nanoparticles for intravascular drug delivery due to sustained release characteristics of polycaprolactone [53]. Despite the recently enhanced interest in essential oil encapsulated PCL nanoparticles, the investigations into the antimicrobial activities of nanoparticulate oil delivery systems are still minimal.

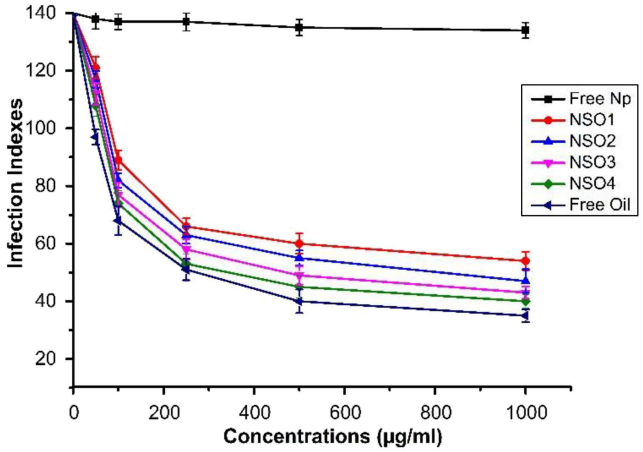

Fig. 8 *Infection indexes of the free NSO, empty PCL NPs, and different concentrations of synthetised NSO encapsulated PCL NPs*

NSO is known as one of the most potent antimicrobial agents and can inhibit several drug sensitive and resistant-bacteria, viruses, fungi and parasites [54, 55]. In our previous study, we examined the antileishmanial efficacies of NSO alone and in a combination with TiO_2-Ag nanoparticles [25]. At first, we determined non-toxic concentrations of NSO and TiAgNps on J774 macrophage cells and it was found that 20, 30, and 50 µg/ml concentrations of NSO were non-toxic. Besides, non-toxic dosages of TiAgNps were evaluated as 10, 15, and 20 µg/ml. By using non-toxic concentrations, combinations including different concentrations of TiAgNps and NSO were prepared. All combinations exhibited significant antileishmanial effect against *L. tropica* promastigotes and amastigotes while the inhibitory efficacies of non-toxic concentrations of NSO remained at lower levels. This indicates improved antileishmanial effectiveness of NSO when supplemented with another influential antimicrobial agent.

Table 2 Amounts of released nitric oxide (nmol/ml) from macrophages treated with oil encapsulated nanoparticle formulations, free oil, and free nanoparticles following to 192 h incubation

	Free Np	Free oil	NSO1	NSO2	NSO3	NSO4
control	4.5 ± 0.31	4.5 ± 0.31	4.5 ± 0.31	4.5 ± 0.31	4.5 ± 0.31	4.5 ± 0.31
50 µg/ml	4.9 ± 0.47	4.6 ± 0.58	5.3 ± 0.38	5.7 ± 0.55	6.0 ± 0.63	6.6 ± 0.61
100 µg/ml	5.0 ± 0.45	4.9 ± 0.29	5.8 ± 0.44	6.8 ± 0.51	7.2 ± 0.66	8.1 ± 0.59
250 µg/ml	5.6 ± 0.38	5.8 ± 0.44	6.9 ± 0.53	7.7 ± 0.65	8.8 ± 0.61	9.5 ± 0.82
500 µg/ml	6.1 ± 0.50	6.3 ± 0.57	8.1 ± 0.63	9.6 ± 0.76	10.9 ± 0.75	11.5 ± 0.81
1000 µg/ml	7.3 ± 0.48	7.4 ± 0.61	10.3 ± 0.74	11.4 ± 0.85	12.8 ± 0.79	13.2 ± 0.91

Considering toxic features and also the high bioactive potency of NSO, we proposed that encapsulation of the mentioned oil into PCL nanoparticles could enhance its antileishmanial activity while decreasing its toxicity. Moreover, we also predicted that further entrapment of NSO into polymeric nanoparticulate delivery systems such as polycaprolactone might increase its water solubility, provide stability within biological systems, protection from degradation and facilitate its cargo into Leishmania-infected cells and tissues.

There are a few studies in the literature regarding encapsulation of NSO into polymeric nanoparticles. In one study on this subject, Doolaanea *et al.* achieved the encapsulation of NSO into biodegradable PLGA nanoparticles with high efficiency [56]. They used 30 mg NSO as initial doses prior to encapsulation and demonstrated that PLGA nanoparticles completely capsulised included oil molecules by using FTIR spectroscopy. In 2016, the same group performed another study in order to investigate neuroregenerative activities of PLGA nanoparticles loaded with NSO and plasmid DNA in combination for developing new gene therapy model against neurodegenerative diseases. They showed that application of co-encapsulated formulations provided extensive and rapid neurite differentiation from neuroblastoma cells when compared with PLGA nanoparticles that did not include NSO [57]. Despite ongoing studies, no research has been performed yet for encapsulation of NSO into PCL nanoparticles and determination of their biological activities. The current study is the first to investigate encapsulation of NSO into PCL nanoparticulate delivery systems and determine their antileishmanial efficacies.

At first, we observed that the mean sizes of oil-loaded nanoparticles were significantly higher than empty nanoparticles according to DLS analysis. This was an important signal indicating efficient encapsulation of oil molecules. The mean sizes of PCL nanoparticles increased when a higher initial concentration of NSO was used. In a similar research, Govender *et al.* provided encapsulation of a water-soluble drug named as procaine dihydrochloride into PLGA nanoparticles by preparing formulations that included different initial amounts of drug molecules. Researchers demonstrated that when percentages of drug content within particles increased from 0.2 to 4.6%, the mean size of nanoparticles expanded from 157 to 209 nm [58]. This indicates that enhanced sizes of drug-loaded nanoparticles directly reflect the amount of drug molecules that are encapsulated into delivery systems and this situation was observed in our current study.

According to the release profiles of oil-loaded nanoparticles, we found that all synthetised nano-formulations released more than 85% of encapsulated oil molecules after 288 h of incubation. It is well known that degradation of PCL polymer is slower than other polymeric nanoparticles such as PLGA and this facilitates the sustained drug release characteristics of PCL-based nanoparticulate delivery systems [29, 59, 60]. In a similar study, Kamaraj *et al.* demonstrated that PCL nanoparticles that were loaded with DDA (14-deoxy-11, 12-didehydroandrographolide), a herbal extract, and released all the encapsulated drug molecules after 300 h of incubation, while the percentages of released drug amounts were measured as only 50% after 100 h of incubation [61]. This result confirms an initially slower release profile of the PCL polymer and indicates that a burst release of the drugs developed at the end of 3–4 days incubation. Since a maximum 30% release of NSO was recorded after 72 h and this rate increased considerably with time, our results are consistent with the data from previous studies.

After characterisation and determination of nano-formulation release profiles, we explored the antileishmanial efficacies of NSO encapsulated PCL nanoparticles on *L. infantum* promastigotes and amastigotes, in vitro. We established that all tested formulations inhibited more than 80% of *L. infantum* promastigotes at 192 h incubation. Furthermore, oil-loaded nanoparticles showed the significant anti-amastigote effect by dramatically suppressing the infection indexes of macrophages. The most considerable antileishmanial effect was observed when the NSO4 formulation was applied since it inhibited more than 80% of *L. infantum* promastigotes and amastigotes after 192 h incubation. Overwhelmingly enhanced anti-promastigote activities of NSO oil-loaded PCL nanoparticles ranging at time intervals between 72 and 192 h can be explained by rapid degradation of the PCL polymer and increased amounts of released oil molecules after 72 h incubation.

Another important result that was obtained by anti-promastigote and anti-amastigote activity assay is that free NSO exhibited higher antileishmanial effectiveness in contrast to oil-loaded nanoparticles within tested time periods. We think that this may be arisen from direct and instant contact of parasites with high dosages of oil molecules, while nanoparticles provided a sustainable release of oil. Therefore, parasites exposed to lower doses of NSO at the beginning when they were faced with loaded nanoparticles even though the same concentrations of free oil and oil encapsulated PCL nanoparticles were applied. Nevertheless, inhibitory effects of the nanoparticulate formulations increased with degradation of the polymer by the time.

Several studies have demonstrated that drug encapsulated nanoparticle formulations displayed similar or lower antimicrobial efficacies in contrast to free drug. In a similar study, Akbari *et al.* found that ciprofloxacin encapsulated niosomes were excellent agents in order to overcome *S.aureus* infections; however, the inhibitory activities of these nanoparticles were two times lower than free drugs [62]. Hence, the determination of approximately similar levels of antileishmanial activities against *L. infantum* promastigotes and amastigotes are consistent with the results of previous studies.

Furthermore, these NSO-loaded PCL nanoparticles are appropriate for drug delivery systems since they show nearly similar inhibitory effects, and they have potential to provide sustained release of oil without any degradation, improving bioavailability and solubility and transportation into Leishmania-infected tissues. All these are advantages of using NSO-loaded PCL nanoparticles compared to free oil.

In the last step of our experiments, we examined the stimulatory roles of synthetised nanoparticles on macrophages to generate NO. NO is known as a notable antileishmanial agent that can directly kill the parasites by binding and disrupting vital parasite enzymes or proteins. Moreover, it can also regulate the release of IFN-gamma and IL-12 that are special cytokines that stimulate a Th1 immune response against parasitic evasion [63]. Therefore, stimulating NO release from macrophages can be considered as a critical performance metric for newly developed antileishmanial compounds that provides complete eradication of the infection via activation of the immune system. Our experiments found that application of NSO encapsulated PCL nanoparticles resulted in a 2–4-fold increase in NO secretion of macrophages in contrast to free oil and empty nanoparticles. As adjuvanicities of NSO oil and PCL polymers were previously proven, the enhanced immunomodulatory effects of NSO encapsulated PCL nanoparticles may be associated with synergistic activities of these two good adjuvants. On the other hand, in vitro macrophage culture systems have some limitations in reflecting the results of in vivo studies. Macrophages can demonstrate wide heterogeneity in in vivo systems. Moreover, transformed cell lines promote some genetic and phenotypical variations in contrast to primary cultures [64–67] Therefore, utilisation of cell lines may not always ascertain accurate considerations for in vivo results.

Consequently, this current study is the first to demonstrate that NSO encapsulated PCL nanoparticles were excellent platforms that possess high encapsulation efficacies, provided sustained and enhanced release of oil molecules with significant antileishmanial effectiveness with extreme inhibition of the growth of *L. infantum* promastigotes and amastigotes. These promising data reveal that PCL-based nanoparticulate delivery systems can be used in the fight against leishmaniasis in the near future subsequent to the determination of their in vivo activities. It is our opinion that such nanoparticulate delivery systems may soon take the place of current antileishmanial drugs.

5 References

[1] Ready, P.D.: 'Epidemiology of visceral leishmaniasis', *Clin. Epidemiol.*, 2014, **6**, pp. 147–154

[2] Das, A., Ali, N.: 'Vaccine development against *Leishmania donovani*', *Front. Immunol.*, 2012, **3**, p. 99

[3] Sundar, S., Chakravarty, J.: 'Liposomal amphotericin B and leishmaniasis: dose and response', *J. Glob. Infect. Dis.*, 2010, **2**, (2), pp. 159–166

[4] Gonzalez, C., Wang, O., Strutz, S.E., *et al.*: 'Climate change and risk of leishmaniasis in North America: predictions from ecological niche models of vector and reservoir species', *PLoS Negl. Trop. Dis.*, 2010, **4**, (1), p. e585

[5] Salomon, O.D., Quintana, M.G., Mastrangelo, A.V., *et al.*: 'Leishmaniasis and climate change-case study: Argentina', *J. Trop. Med.*, 2012, **2012**, p. 601242

[6] Stamm, L.V.: 'Human migration and leishmaniasis-on the move', *JAMA Dermatol.*, 2016, **152**, (4), pp. 373–374

[7] Alawieh, A., Musharrafieh, U., Jaber, A., *et al.*: 'Revisiting leishmaniasis in the time of war: the Syrian conflict and the Lebanese outbreak', *Int. J. Infect. Dis.*, 2014, **29**, pp. 115–119

[8] Hayani, K., Dandashli, A., Weisshaar, E.: 'Cutaneous leishmaniasis in Syria, clinical features, current status and the effects of war', *Acta Derm. Venereol.*, 2015, **95**, (1), pp. 62–66

[9] Kedzierski, L.: 'Leishmaniasis vaccine: where are we today?', *J. Glob. Infect. Dis.*, 2010, **2**, (2), pp. 177–185

[10] Sundar, S., Singh, A., Singh, O.P.: 'Strategies to overcome antileishmanial drugs unresponsiveness', *J. Trop. Med.*, 2014, **2014**, p. 646932

[11] de Menezes, J.P., Guedes, C.E., Petersen, A.L., *et al.*: 'Advances in development of new treatment for leishmaniasis', *BioMed Res. Int.*, 2015, **2015**, p. 815023

[12] Rates, S.M.K.: 'Plants as source of drugs', *Toxicon*, 2001, **39**, (5), pp. 603–613

[13] Rosa, M.D.S., Mendonca, R.R., Bizzo, H.R., *et al.*: 'Antileishmanial activity of a linalool-rich essential oil from *Croton cajucara*', *Antimicrob. Agents Chemother.*, 2003, **47**, (6), pp. 1895–1901

[14] Garcia, M., Scull, R., Satyal, P., *et al.*: 'Chemical characterization, antileishmanial activity, and cytotoxicity effects of the essential oil from leaves of *Pluchea carolinensis* (Jacq.) G. Don. (Asteraceae)', *Phytother. Res.*, 2017, **31**, pp. 1419–1426

[15] Burt, S.: 'Essential oils: their antibacterial properties and potential applications in foods – a review', *Int. J. Food Microbiol.*, 2004, **94**, (3), pp. 223–253

[16] Helander, I.M., Alakomi, H.L., Latva-Kala, K., *et al.*: 'Characterization of the action of selected essential oil components on gram-negative bacteria', *J. Agric. Food Chem.*, 1998, **46**, (9), pp. 3590–3595

[17] Ultee, A., Bennik, M.H.J., Moezelaar, R.: 'The phenolic hydroxyl group of Carvacrol is essential for action against the food-borne pathogen *Bacillus cereus*', *Appl. Environ. Microbiol.*, 2002, **68**, (4), pp. 1561–1568

[18] Tariku, Y., Hymete, A., Hailu, A., *et al.*: 'Essential-oil composition, antileishmanial, and toxicity study of *Artemisia abyssinica* and *Satureja punctata* Ssp Punctata front Ethiopia', *Chem. Biodiversity*, 2010, **7**, (4), pp. 1009–1018

[19] Essid, R., Rahali, F.Z., Msaada, K., *et al.*: 'Antileishmanial and cytotoxic potential of essential oils from medicinal plants in Northern Tunisia', *Ind. Crops Prod.*, 2015, **77**, pp. 795–802

[20] Randhawa, M.A., Alghamdi, M.S.: 'Anticancer activity of *Nigella sativa* (black seed) – a review', *Am. J. Chin. Med.*, 2011, **39**, (6), pp. 1075–1091

[21] Ahmad, A., Husain, A., Mujeeb, M., *et al.*: 'A review on therapeutic potential of *Nigella sativa*: a miracle herb', *Asian Pac. J. Trop. Biomed.*, 2013, **3**, (5), pp. 337–352

[22] Boskabady, M.H., Mohsenpoor, N., Takaloo, L.: 'Antiasthmatic effect of *Nigella sativa* in airways of asthmatic patients', *Phytomedicine*, 2010, **17**, (10), pp. 707–713

[23] Elmowalid, G., Amar, A.M., Ahmad, A.A.: '*Nigella sativa* seed extract: 1. Enhancement of sheep macrophage immune functions in vitro', *Res. Vet. Sci.*, 2013, **95**, (2), pp. 437–443

[24] Mahmoudvand, H., Tavakoli, R., Sharififar, F., *et al.*: 'Leishmanicidal and cytotoxic activities of *Nigella sativa* and its active principle, Thymoquinone', *Pharm. Biol.*, 2015, **53**, (7), pp. 1052–1057

[25] Abamor, E.S., Allahverdiyev, A.M.: 'A nanotechnology based new approach for chemotherapy of Cutaneous Leishmaniasis: Tio2@Ag nanoparticles – *Nigella sativa* oil combinations', *Exp. Parasitol.*, 2016, **166**, pp. 150–163

[26] Yap, P.S., Yiap, B.C., Ping, H.C., *et al.*: 'Essential oils, a new horizon in combating bacterial antibiotic resistance', *Open Microbiol. J.*, 2014, **8**, pp. 6–14

[27] Bonifacio, B.V., Silva, P.B., Ramos, M.A., *et al.*: 'Nanotechnology-based drug delivery systems and herbal medicines: a review', *Int. J. Nanomedicine*, 2014, **9**, pp. 1–15

[28] Kumar, M.N.V.R.: 'Nano and microparticles as controlled drug delivery devices', *J. Pharmacy Pharm. Sci.*, 2000, **3**, (2), pp. 234–258

[29] Danafar, H.: 'MPEG–PCL Copolymeric nanoparticles in drug delivery systems', *Cogent Med.*, 2016, **3**, p. 1142411

[30] Mansour, H.M., Sohn, M., Al-Ghananeem, A., *et al.*: 'Materials for pharmaceutical dosage forms: molecular pharmaceutics and controlled release drug delivery aspects', *Int. J. Mol. Sci.*, 2010, **11**, (9), pp. 3298–3322

[31] Peng, W., Jiang, X.Y., Zhu, Y., *et al.*: 'Oral delivery of capsaicin using MPEG-PCL nanoparticles', *Acta Pharmacol. Sin.*, 2015, **36**, (1), pp. 139–148

[32] Nguyen, M.K., Alsberg, E.: 'Bioactive factor delivery strategies from engineered polymer hydrogels for therapeutic medicine', *Prog. Polym. Sci.*, 2014, **39**, (7), pp. 1236–1265

[33] Kumari, A., Yadav, S.K., Yadav, S.C.: 'Biodegradable polymeric nanoparticles based drug delivery systems', *Colloids Surf. B, Biointerfaces*, 2010, **75**, (1), pp. 1–18

[34] Elcicek, S., Bagirova, M., Allahverdiyev, A.M.: 'Generation of avirulent leishmania parasites and induction of nitric oxide production in macrophages by using polyacrylic acid', *Exp. Parasitol.*, 2013, **133**, (3), pp. 237–242

[35] Perricone, M., Arace, E., Corbo, M.R., *et al.*: 'Bioactivity of essential oils: a review on their interaction with food components', *Front. Microbiol.*, 2015, **6**, p. 76

[36] Sharifi-Rad, J., Hoseini-Alfatemi, S.M., Sharifi-Rad, M., *et al.*: 'Antibacterial, antioxidant, antifungal and anti-inflammatory activities of crude extract from *Nitraria schoberi* fruits', *3 Biotech.*, 2015, **5**, (5), pp. 677–684

[37] Prabuseenivasan, S., Jayakumar, M., Ignacimuthu, S.: 'In vitro antibacterial activity of some plant essential oils', *BMC Complement. Altern. Med.*, 2006, **6**, p. 39

[38] Sherry, M., Charcosset, C., Fessi, H., *et al.*: 'Essential oils encapsulated in liposomes: a review', *J. Liposome Res.*, 2013, **23**, (4), pp. 268–275

[39] Martin, A., Verona, S., Navarrete, A., *et al.*: 'Encapsulation and co-precipitation processes with supercritical fluids: applications with essential oils', *Open Chem. Eng. J.*, 2010, **4**, pp. 31–41

[40] Coimbra, M., Isacchi, B., van Bloois, L., *et al.*: 'Improving solubility and chemical stability of natural compounds for medicinal use by incorporation into liposomes', *Int. J. Pharm.*, 2011, **416**, (2), pp. 433–442

[41] Saviuc, C., Grumezescu, A.M., Chifiriuc, C.M., *et al.*: 'Hybrid nanosystem for stabilizing essential oils in biomedical applications', *Dig. J. Nanomater. Biostruct.*, 2011, **6**, (4), pp. 1657–1666

[42] Yousefzadi, M., Ebrahimi, S.N., Sonboli, A., *et al.*: 'Cytotoxicity, antimicrobial activity and composition of essential oil from *Tanacetum balsamita* L. Subsp. Balsamita', *Nat. Prod. Commun.*, 2009, **4**, (1), pp. 119–122

[43] Sinha, S., Jothiramajayam, M., Ghosh, M., *et al.*: 'Evaluation of toxicity of essential oils Palmarosa, Citronella, Lemongrass and Vetiver in human lymphocytes', *Food Chem. Toxicol.*, 2014, **68**, pp. 71–77

[44] Adukwu, E.C., Bowles, M., Edwards-Jones, V., *et al.*: 'Antimicrobial activity, cytotoxicity and chemical analysis of lemongrass essential oil (*Cymbopogon flexuosus*) and pure citral', *Appl. Microbiol. Biotechnol.*, 2016, **100**, (22), pp. 9619–9627

[45] Hsieh, W.C., Chang, C.P., Gao, Y.L.: 'Controlled release properties of chitosan encapsulated volatile citronella oil microcapsules by thermal treatments', *Colloids Surf. B, Biointerfaces*, 2006, **53**, (2), pp. 209–214

[46] Ortan, A., Campeanu, G., Dinu-Pirvu, C., *et al.*: 'Studies concerning the entrapment of Anethum Graveolens essential oil in liposomes', *Romanian Biotechnol. Lett.*, 2009, **14**, (3), pp. 4413–4419

[47] Noh, Y.W., Hong, J.H., Shim, S.M., *et al.*: 'Polymer nanomicelles for efficient mucus delivery and antigen-specific high mucosal immunity', *Angew. Chem. Int. Ed. Engl.*, 2013, **52**, (30), pp. 7684–7689

[48] Sutton, D., Nasongkla, N., Blanco, E., *et al.*: 'Functionalized micellar systems for cancer targeted drug delivery', *Pharm. Res.*, 2007, **24**, (6), pp. 1029–1046

[49] Barua, S., Mitragotri, S.: 'Challenges associated with penetration of nanoparticles across cell and tissue barriers: a review of current status and future prospects', *Nano. Today*, 2014, **9**, (2), pp. 223–243

[50] Joseph, E., Saha, R.N.: 'Advances in brain targeted drug delivery: nanoparticulate systems', 2013, 3

[51] Choi, M.J., Soottitantawat, A., Nuchuchua, O., *et al.*: 'Physical and light oxidative properties of Eugenol encapsulated by molecular inclusion and emulsion-diffusion method', *Food Res. Int.*, 2009, **42**, (1), pp. 148–156

[52] Ephrem, E., Greige-Gerges, H., Fessi, H., *et al.*: 'Optimisation of Rosemary oil encapsulation in polycaprolactone and scale-up of the process', *J. Microencapsul.*, 2014, **31**, (8), pp. 746–753

[53] Thonggoom, O., Punrattanasin, N., Srisawang, N., *et al.*: 'In vitro controlled release of clove essential oil in self-assembly of amphiphilic polyethylene glycol-block-polycaprolactone', *J. Microencapsul.*, 2016, **33**, (3), pp. 239–248

[54] Emeka, L.B., Emeka, P.M., Khan, T.M.: 'Antimicrobial activity of *Nigella sativa* L. Seed oil against multi-drug resistant *Staphylococcus aureus* isolated from diabetic wounds', *Pak. J. Pharm. Sci.*, 2015, **28**, (6), pp. 1985–1990

[55] Barakat, E.M., El Wakeel, L.M., Hagag, R.S.: 'Effects of *Nigella sativa* on outcome of hepatitis C in Egypt', *World J. Gastroenterol.*, 2013, **19**, (16), pp. 2529–2536

[56] Doolaanea, A.A., Harun, A.F., Mohamed, F.: 'Quantification of *Nigella sativa* oil (NSO) from biodegradable PLGA nanoparticles using FTIR spectroscopy', *Int. J. Pharm. Pharm. Sci.*, 2014, **6**, (10), pp. 228–232

[57] Doolaanea, A.A., Mansor, N., Mohd Nor, N.H., *et al.*: 'Co-encapsulation of *Nigella sativa* oil and plasmid DNA for enhanced gene therapy of Alzheimer's disease', *J. Microencapsul.*, 2016, **33**, (2), pp. 114–126

[58] Govender, T., Stolnik, S., Garnett, M.C., *et al.*: 'PLGA nanoparticles prepared by nanoprecipitation: drug loading and release studies of a water soluble drug', *J. Control. Release*, 1999, **57**, (2), pp. 171–185

[59] Abedalwafa, M., Wang, F.J., Wang, L., *et al.*: 'Biodegradable poly-epsilon-caprolactone (Pcl) for tissue engineering applications: a review', *Rev. Adv. Mater. Sci.*, 2013, **34**, (2), pp. 123–140

[60] Azimi, B., Nourpanah, P., Rabiee, M., *et al.*: 'Poly (Epsilon-Caprolactone) fiber: an overview', *J. Eng. Fibers Fabr.*, 2014, **9**, (3), pp. 74–90

[61] Kamaraj, N., Yashwanthi, P., Isaac, P.K., *et al.*: 'Fabrication, characterization, in vitro drug release and glucose uptake activity of 14-Deoxy, 11, 12-didehydroandrographolide loaded polycaprolactone nanoparticles', *Asian J. Pharm. Sci.*, 2017, **12**, (4), pp. 353–362

[62] Akbari, V., Abedi, D., Pardakhty, A., *et al.*: 'Release studies on ciprofloxacin loaded non-ionic surfactant vesicles', *Avicenna. J. Med. Biotechnol.*, 2015, **7**, (2), pp. 69–75

[63] Gutierrez, F.R., Mineo, T.W., Pavanelli, W.R., *et al.*: 'The effects of nitric oxide on the immune system during *Trypanosoma cruzi* infection', *Mem. Inst. Oswaldo Cruz*, 2009, **104**, Suppl. 1, pp. 236–245

[64] Burdall, S.E., Hanby, A.M., Lansdown, M.R.J., *et al.*: 'Breast cancer cell lines: friend or foe?', *Breast Cancer Res.*, 2003, **5**, pp. 89–95

[65] Pan, C., Kumar, C., Bohl, S., *et al.*: 'Comparative proteomic phenotyping of cell lines and primary cells to assess preservation of cell type-specific functions', *Mol. Cell. Proteomics, MCP*, 2009, **8**, pp. 443–450

[66] Frattini, A., Fabbri, M., Valli, R., *et al.*: 'High variability of genomic instability and gene expression profiling in different HeLa clones', *Sci. Rep.*, 2015, **20**, (5), p. 15377

[67] Andreu, N., Phelan, J., de Sessions, P.F., *et al.*: 'Primary macrophages and J774 cells respond differently to infection with *Mycobacterium tuberculosis*', *Sci. Rep.*, 2017, **8**, (7), p. 42225